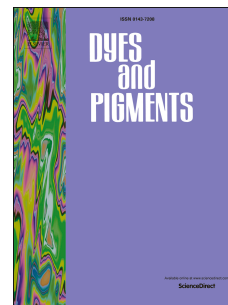


Journal Pre-proof

Three anthracene-based bis-imidazolium salts: Synthesis, structure and recognition for 2,4-dinitrophenylhydrazine

Qingxiang Liu, Shaocong Yu, Zhixiang Zhao, Xiantao Zhang, Rui Liu



PII: S0143-7208(19)31968-0

DOI: <https://doi.org/10.1016/j.dyepig.2019.107983>

Reference: DYPI 107983

To appear in: *Dyes and Pigments*

Received Date: 20 August 2019

Revised Date: 12 October 2019

Accepted Date: 18 October 2019

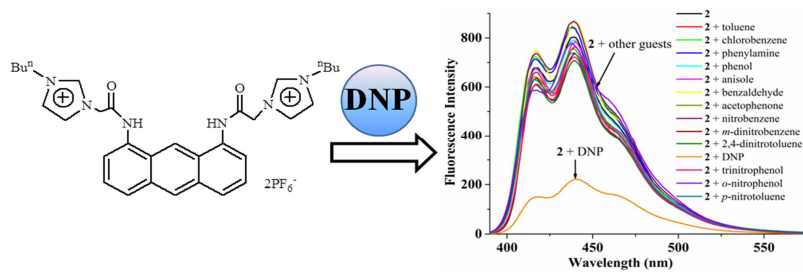
Please cite this article as: Liu Q, Yu S, Zhao Z, Zhang X, Liu R, Three anthracene-based bis-imidazolium salts: Synthesis, structure and recognition for 2,4-dinitrophenylhydrazine, *Dyes and Pigments* (2019), doi: <https://doi.org/10.1016/j.dyepig.2019.107983>.

This is a PDF file of an article that has undergone enhancements after acceptance, such as the addition of a cover page and metadata, and formatting for readability, but it is not yet the definitive version of record. This version will undergo additional copyediting, typesetting and review before it is published in its final form, but we are providing this version to give early visibility of the article. Please note that, during the production process, errors may be discovered which could affect the content, and all legal disclaimers that apply to the journal pertain.

© 2019 Published by Elsevier Ltd.

Graphic abstract:

Anthracene-based bis-imidazolium salts **1-3** have been prepared. The recognition of **2** (or **3**) for 2,4-dinitrophenylhydrazine was investigated.



Three Anthracene-based Bis-imidazolium Salts: Synthesis, Structure and Recognition for 2,4-Dinitrophenylhydrazine

Qingxiang Liu,^{*} Shaocong Yu, Zhixiang Zhao, Xiantao Zhang and Rui Liu

Tianjin Key Laboratory of Structure and Performance for Functional Molecules, MOE Key Laboratory of Inorganic-Organic Hybrid Functional Material Chemistry, College of Chemistry, Tianjin Normal University, Tianjin 300387, P. R. China.

** Corresponding author, E-mail: tjnulqx@163.com*

Abstract

Three anthracene-based bis-imidazolium salts 1,8-bis[2'-(*N*-R-imidazoliumyl)acetamido]anthracene 2X (**1**: R = ⁿBu, X = Cl⁻; **2**: R = ⁿBu, X = PF₆⁻; **3**: R = Et, X = PF₆⁻) were prepared. The structure of **1** was demonstrated by X-ray analysis. The selective recognition of **2** (or **3**) for some aromatic compounds (toluene, chlorobenzene, phenylamine, phenol, anisole, benzaldehyde, acetophenone, nitrobenzene, *m*-dinitrobenzene, 2,4-dinitrotoluene, 2,4-dinitrophenylhydrazine (DNP), trinitrophenol, *o*-nitrophenol, *p*-nitrotoluene) was investigated through fluorescence, ultraviolet, ¹H NMR, HRMS and IR spectra at 25 °C. Compounds **2** (or **3**) showed good selective recognition ability for DNP, and they could effectively distinguish DNP from other aromatic compounds. The association constants and detection limits of **2** and **3** were similar, which displayed sizes of side chains (ⁿBu for **2** and Et for **3**) had no remarkable effect on the recognition of DNP.

Keywords: bis-imidazolium; fluorescence; recognition; 2,4-dinitrophenylhydrazine

1. Introduction

Selective recognition and sensing of aromatic compounds occupy an important position in the field of fluorescence recognition because some aromatic compounds are serious environmental pollutants [1-5]. As is known to all, aromatic compounds

are poisonous to humans and animals, and they can cause some diseases, such as cancer [6-9]. What's more, they can also infiltrate into biological ecosystem through direct discharge of industrial castoffs [10-12]. The detection methods of aromatic compounds contain LC-MS, GC-MS, HPLC [13-20]. In these methods, the fluorescence method is widely used due to its sensitivity and speediness [21-31]. Therefore, it is necessary to develop more sensitive and efficient fluorescence chemosensors for aromatic compounds.

In order to search for suitable chemosensors toward the detection of aromatic compounds, we became interested in anthracene-based bis-imidazolium salts. In this work, the synthesis of three bis-imidazolium salts 1,8-bis[2'-(*N*-R-imidazoliumyl)acetamido]anthracene 2X (**1**: R = ⁿBu, X = Cl⁻; **2**: R = ⁿBu, X = PF₆⁻; **3**: R = Et, X = PF₆⁻) was reported. The structure of **1** was demonstrated through X-ray analysis. The selective detection of **2** (or **3**) for some aromatic compounds (toluene, chlorobenzene, phenylamine, phenol, anisole, benzaldehyde, acetophenone, nitrobenzene, *m*-dinitrobenzene, 2,4-dinitrotoluene, 2,4-dinitrophenylhydrazine (DNP), trinitrophenol, *o*-nitrophenol, *p*-nitrotoluene) was investigated through fluorescence, ultraviolet, ¹H NMR, HRMS and IR spectra in acetonitrile at 25 °C.

2. Experimental

2.1. General

The reagents of analytical grade were used in tests and preparations. A Varian Mercury Vx 400 spectrometer was employed for the measurement of ¹H NMR and ¹³C NMR spectra. A Boetius Block apparatus was used for the determination of melting points. A Perkin-Elmer 2400C Elemental Analyzer was used for the measurement of elemental analyses. A Cary Eclipse fluorescence spectrophotometer was employed for the measurement of fluorescence spectra. A Bruker Equinox 55 spectrometer was used for the measurement of IR spectra (KBr). A VG ZAB-HS mass spectrometer (VG, U.K.) was employed for the determination of EI mass spectra. The diffraction data of **1** was collected through a Bruker Apex II CCD diffractometer [32]. The SHELXS program was used to solve the structure of **1** [33]. Crystal-Maker was

employed to form Fig. 1 [34]. Crystallographic data of **1** were listed in Table S1.

2.2. 1,8-Diaminoanthraquinone

Na₂S (3.512 g, 45.0 mmol) and NaOH (4.280 g, 107.0 mmol) were dissolved in water (190 mL) with stirring for 0.5 h, and then EtOH (112 mL) solution of 1,8-dinitroanthraquinone (2.952 g, 9.9 mmol) was added to above solution under refluxing for 6 h. When the solution was cooled to 20 °C, the purple precipitate was generated. The purple powder of 1,8-diaminoanthraquinone was collected by filtration. Yield: 2.320 g (98%). M.p.: 274-275 °C. ¹H NMR (400 MHz, DMSO-*d*₆): δ 7.16 (d, *J* = 9.2 Hz, 2H, AnH), 7.36 (d, *J* = 8.4 Hz, 2H, AnH), 7.45 (t, *J* = 8.0 Hz, 2H, AnH), 7.86 (s, 4H, NH₂).

2.3. 1,8-Diaminoanthracene

1,8-Diaminoanthraquinone (2.000 g, 8.4 mmol) and NaOH (0.072 g, 1.8 mmol) were dissolved in *i*-propanol (100 mL), and then sodium borohydride (4.009 g, 106.0 mmol) was added under N₂. The suspension was heated to reflux for 24 h. After adding 250 mL of ice water, a yellow-green powder of 1,8-diaminoanthracene was precipitated, and the product was collected via filtration. Yield: 1.680 g (96%). M.p.: 175-176 °C. ¹H NMR (400 MHz, DMSO-*d*₆): δ 5.870 (s, 4H, NH₂), 6.55 (t, *J* = 4.1 Hz, 2H, AnH), 7.19 (d, *J* = 4.1 Hz, 4H, AnH), 8.17 (s, 1H, AnH), 8.80 (s, 1H, AnH).

2.4. 1,8-Dichloroacetamidoanthracene

To the dichloromethane solution (150 mL) of triethylamine (2.337 g, 23.1 mmol) and 1,8-diaminoanthracene (2.060 g, 9.6 mmol) was added dropwise chloroacetyl chloride (2.608 g, 23.1 mmol) at 0 °C. Then the mixture was stirred overnight at 25 °C to form a yellow precipitate. The precipitate was collected via filtration and purified by washing with dichloromethane to give a celadon powder of 1,8-dichloroacetamidoanthracene. Yield: 3.400 g (98%). M.p.: > 320 °C. ¹H NMR (400 MHz, DMSO-*d*₆): δ 4.55 (s, 4H, CH₂), 7.56 (q, *J* = 5.2 Hz, 2H, AnH), 7.72 (d, *J* = 6.8 Hz, 2H, AnH), 8.01 (d, *J* = 8.5 Hz, 2H, AnH), 8.68 (s, 1H, AnH), 8.87 (s, 1H, AnH), 10.53 (s, 2H, NH).

2.5. 1,8-Bis[2'-(*N*-*n*-butyl-imidazoliumyl)acetamido]anthracene chloride (**1**) and

*1,8-bis[2'-(*N*-ⁿbutyl-imidazoliumyl)acetamido]anthracene hexafluorophosphate (2)*

A 1,4-dioxane (100 mL) solution of *N*-ⁿbutyl-imidazole (1.029 g, 8.3 mmol) and 1,8-dichloroacetamidoanthracene (1.010 g, 2.8 mmol) was heated to reflux with stirring for 5 days to give a yellow-green solid. 1,8-Bis[2'-(*N*-ⁿbutyl-imidazoliumyl)acetamido]anthracene chloride (**1**) was obtained by filtration and washed with 1,4-dioxane (30 mL). Yield: 1.400 g (82%). M.p.: 276-280 °C. Anal. Calcd for C₃₂H₃₈N₆O₂Cl₂: C, 63.04; H, 6.28; N, 13.78%. Found: C, 63.22; H, 6.31; N, 13.62%. ¹H NMR (400 MHz, DMSO-*d*₆): δ 0.92 (t, *J* = 7.4 Hz, 6H, CH₃), 1.29 (m, 4H, CH₂), 1.83 (m, 4H, CH₂), 4.27 (t, *J* = 7.1 Hz, 4H, CH₂), 5.80 (s, 4H, CH₂), 7.54 (t, *J* = 7.9 Hz, 2H, AnH), 7.87 (s, 2H, ArH), 7.97 (t, *J* = 9.4 Hz, 4H, ArH), 8.04 (d, *J* = 7.3 Hz, 2H, AnH), 8.65 (s, 1H, AnH), 9.43 (s, 2H, imiH), 9.91 (s, 1H, AnH), 11.34 (s, 2H, NH) (imi = imidazole).

The methanol solution (100 mL) of compound **1** (2.194 g, 3.6 mmol) and NH₄PF₆ (1.760 g, 10.8 mmol) were stirred at room temperature for two days. A deep yellow powder was formed, and the powder was collected via filtration and purified by washing with 5 mL of methanol to afford 1,8-bis[2'-(*N*-ⁿbutyl-imidazoliumyl)acetamido]anthracene hexafluorophosphate (**2**). Yield: 1.998 g (67%). M.p.: 194-198 °C. Anal. Calcd for C₃₂H₃₈N₆O₂P₂F₁₂: C, 46.38; H, 4.62; N, 10.14%. Found: C, 46.27; H, 4.58; N, 10.22%. ¹H NMR (400 MHz, DMSO-*d*₆): δ 0.93 (t, *J* = 7.3 Hz, 6H, CH₃), 1.28 (q, *J* = 7.4 Hz, 4H, CH₂), 1.85 (q, *J* = 7.2 Hz, 4H, CH₂), 4.27 (t, *J* = 6.8 Hz, 4H, CH₂), 5.80 (s, 4H, CH₂), 7.54 (t, *J* = 7.9 Hz, 2H, AnH), 7.87 (s, 2H, imiH), 7.93 (d, *J* = 8.4 Hz, 2H, AnH), 7.97 (s, 2H, imiH), 8.04 (d, *J* = 7.2 Hz, 2H, AnH), 8.64 (s, 1H, AnH), 9.42 (s, 2H, imiH), 9.90 (s, 1H, AnH), 11.02 (s, 2H, NH). ¹³C NMR (100 MHz, DMSO-*d*₆): δ 164.77 (C=O), 139.23 (imi-NCN), 137.48, 137.41, 132.96, 131.65, 127.08, 125.55, 125.38, 125.20, 124.11, 124.00, 121.91, 119.48, 116.94 (ArC), 51.73, 48.71, 31.34, 18.74 (CH₂), 13.22 (CH₃).

2.6. *1,8-Bis[2'-(*N*-ethyl-imidazoliumyl)acetamido]anthracene hexafluorophosphate (3)*

Compound **3** was prepared in the analogous method of **2**. Yield: 2.224 g (80%). M.p.: 238-240 °C. Anal. Calcd for C₂₈H₃₀N₆O₂P₂F₁₂: C, 43.53; H, 3.91; N, 10.87%.

Found: C, 43.45; H, 3.82; N, 10.76%. ^1H NMR (400 MHz, DMSO- d_6): δ 1.47 (t, J = 7.1 Hz, 6H, CH_3), 4.28 (q, J = 6.8 Hz, 4H, CH_2), 5.55 (s, 4H, CH_2), 7.57 (t, J = 7.0 Hz, 2H, AnH), 7.86 (q, J = 6.5 Hz, 6H, ArH), 8.00 (d, J = 8.5 Hz, 2H, AnH), 8.69 (s, 1H, AnH), 9.19 (s, 1H, AnH), 9.31 (s, 2H, imiH), 10.90 (s, 2H, NH). ^{13}C NMR (100 MHz, DMSO- d_6): δ 164.74 (C=O), 139.26 (imi-NCN), 137.12, 137.05, 133.35, 132.79, 131.68, 127.16, 125.70, 125.52, 124.07, 123.97, 121.86, 121.68, 121.62, 120.55, 120.18, 116.84 (ArC), 51.54, 44.47, 44.37 (CH_2), 15.06 (CH_3).

2.7. Fluorescence titrations

The stock solutions of chemosensor **2** (or **3**) (1.0×10^{-3} M or 1.0×10^{-4} M) and guests were prepared in CH_3CN . Test solutions were prepared via mixing the solutions of **2** (or **3**) (1.0×10^{-5} M) and guests ($0\text{-}45.0 \times 10^{-5}$ M). The sample solutions were excited at 381 nm for **2** and 383 nm for **3**, and the slits were 5 and 3 nm. And the spectra were recorded from 390 nm to 550 nm.

2.8. Method for Job's Plot

The guest (DNP) and **2** (or **3**) were dissolved in CH_3CN in the concentration of 1×10^{-4} M respectively to prepare a stock solution and the overall concentration remained 1×10^{-5} M in the test solutions, and the molar ratios of $C_{\text{host}}/C_{\text{guest}}$ changed from 1:0 to 0:1. The sample solutions were excited at 381 nm for **2** and 383 nm for **3**, and the slits were 5 nm and 3 nm. And the spectra were recorded from 390 nm to 550 nm.

3. Results and Discussion

3.1. Preparation and characterization of compounds 1-3

As shown in Scheme 1, 1,8-dinitroanthraquinone was reduced by Na_2S in the presence of NaOH to afford 1,8-diaminoanthraquinone, which further reacted with sodium borohydride to form 1,8-diaminoanthracene. Chloroacetyl chloride reacted with 1,8-diaminoanthracene in the presence of Et_3N in CH_2Cl_2 to give 1,8-dichloroacetamidoanthracene, followed reaction with 1- n -butylimidazole in 1,4-dioxane to afford 1,8-bis[2'-(N - n -Bu-imidazoliumyl)acetylamino]anthracene chloride (**1**). The reaction of NH_4PF_6 with **1** in methanol generated 1,8-bis[2'-(N - n -Bu-imidazoliumyl)acetylamino]anthracene hexafluorophosphate (**2**).

Compound **3** was prepared with an analogous to the method of **2**. In the ^1H NMR spectra, the imidazolium proton signals (NCHN) appear at 9.31-9.43 ppm for **1-3** [35-39].

Scheme 1. Preparation of compounds **1-3**.

3.2. Structure of **1**

The single crystal of **1** was obtained by slow diffusion of diethyl ether into its CH_3CN solution, and the structure of **1** was demonstrated by X-ray analysis. In the crystal structure of **1** (Fig. 1), the angle of N-C-N in the imidazole ring was $108.3(4)^\circ$, which was similar to those of the known imidazolium salts [39-40]. Two imidazole rings in **1** were parallel, and they formed the dihedral angles of $71.4(3)^\circ$ with anthracene ring. In Fig. S1, 1D polymeric chain of **1** was generated through C-H \cdots Cl hydrogen bonds [41], in which hydrogen atoms were from methylene on both flanks of imidazole ring (Table S2).

Fig. 1. Crystal structure of **1**. Selected bond lengths (\AA) and angles ($^\circ$): O(1)-C(15) 1.216(5), N(1)-C(15) 1.423(7), N(2)-C(19) 1.320(7), N(3)-C(19) 1.330(6); N(2)-C(19)-N(3) $108.3(4)$. Symmetric code: $i = x, 1 + y, z$.

3.3. Recognition of 2,4-dinitrophenylhydrazine (DNP) using **2** as a host

Compounds **1** and **2** have the same cationic moiety, and different anionic moieties (Cl^- for **1** and PF_6^- for **2**). As shown in Fig. S2, the fluorescence intensity of **1** is weaker than that of **2** due to the influence of different anions. To avoid the interference of chloride ion, we chose **2** as a host to study the selective recognition of some aromatic compounds (toluene, phenylamine, chlorobenzene, anisole, phenol, acetophenone, benzaldehyde, nitrobenzene, *m*-dinitrobenzene, 2,4-dinitrotoluene, 2,4-dinitrophenylhydrazine (DNP), trinitrophenol, *o*-nitrophenol and *p*-nitrotoluene) in CH_3CN at 25°C .

The free **2** (1.0×10^{-5} M) exhibited strong triple emission peak at 390-550 nm as

displayed in Fig. 2 ($\lambda_{\text{ex}} = 381$ nm, emission and excitation slits: 3 nm and 5 nm), and this peak was attributed to the emission of anthracene. No significant change was observed after adding 10 equiv. of toluene, chlorobenzene, phenylamine, phenol, anisole, benzaldehyde, acetophenone, nitrobenzene, *m*-dinitrobenzene, 2,4-dinitrotoluene, trinitrophenol, *o*-nitrophenol, *p*-nitrotoluene. However, adding the same amount of 2,4-dinitrophenylhydrazine (DNP) caused a remarkable decrease of the emission intensity.

Fig. 3 showed the fluorescence spectra of **2** after adding different concentrations of DNP. When the C_{DNP} enhanced gradually, the intensity of emission of **2** at 390-550 nm decreased fastly as displayed in the inset of Fig. 3. When the ratio of C_{DNP}/C_2 exceeded 1:1, the rate of decreasing of fluorescence intensity changed slowly. Finally, the intensity of emission peaks no longer changed when C_{DNP}/C_2 surpassed 30. The quenching behaviors of 2,4-dinitrophenylhydrazine on the fluorescence of **2** were found to fit well with the traditional Stern-Volmer relationship (eqn (1)) [42].

$$F_0/F = 1 + K_{\text{SV}}C_{\text{DNP}} \quad (1)$$

in which F and F_0 expressed the intensities of **2** with or without DNP, C_{DNP} represented the concentration of DNP, and the K_{SV} was the association constant. This equation revealed that F_0/F enhances in direct proportion to the enhancing C_{DNP} .

The quenching constant K_{SV} was computed as $5.6 \times 10^4 \text{ M}^{-1}$ ($R = 0.999$) for **2**·DNP by employing the equation (1), and the linear portion was in the ranges of $0-4.5 \times 10^{-4} \text{ M}$ as shown in Fig. S3. As displayed in Fig. S4, the intensity data were normalized between the minimum intensity and the maximum intensity, and the concentrations of DNP were in the ranges of $0-0.019 \mu\text{M}$. A linear regression curve was fitted to the seven points. By calculating ratio between 3σ and k , the detection limit (LOD) was computed as $3.97 \times 10^{-10} \text{ mol}\cdot\text{L}^{-1}$ for **2** ($\text{LOD} = 3\sigma/k$, σ was the blank standard deviation and k was the slope of the linear regression curve) [43,44]. This result was even lower than the lowest value of literatures ($10^{-7}-10^{-9} \text{ mol}\cdot\text{L}^{-1}$) [45,46]. The complexation stoichiometry between **2** and DNP was established by using the Job's plot method (Fig. S5). When molar fraction (χ) of **2** was 0.5, the $\chi\Delta I$ value for **2**·DNP reached maximum, which indicated the complexation stoichiometry

between **2** and DNP was 1:1 [47-49].

To test recognition ability of **2** for DNP in the existence of other aromatic compounds, the competition experiments were carried out. Firstly, compound **2** ($1.0 \times 10^{-5} \text{ mol}\cdot\text{L}^{-1}$) was mixed with various aromatic compounds (toluene, chlorobenzene, phenylamine, phenol, anisole, benzaldehyde, acetophenone, nitrobenzene, *m*-dinitrobenzene, 2,4-dinitrotoluene, trinitrophenol, *o*-nitrophenol, *p*-nitrotoluene) in the concentration of $1.0 \times 10^{-4} \text{ mol}\cdot\text{L}^{-1}$, and then added the 10 equiv. of 2,4-dinitrophenylhydrazine. Using fluorescent spectra to monitor the competition experiments, no obvious interference was observed except *p*-nitrotoluene and trinitrophenol (Fig. S6). After adding *p*-nitrotoluene and trinitrophenol, the fluorescence intensity increased about 8-10% than that in the existence of 2,4-dinitrophenylhydrazine alone. These results showed that compound **2** was able to effectively discriminate 2,4-dinitrophenylhydrazine from other aromatic compounds.

Fig. 2. Fluorescence spectra of **2** ($1 \times 10^{-5} \text{ mol}\cdot\text{L}^{-1}$) in the presence of guest molecules (chlorobenzene, toluene, phenylamine, anisole, phenol, acetophenone, benzaldehyde, nitrobenzene, *m*-dinitrobenzene, 2,4-dinitrotoluene, 2,4-dinitrophenylhydrazine (DNP), trinitrophenol, *o*-nitrophenol, *p*-nitrotoluene) (10 equiv. for each guest) in CH_3CN at 25 °C. ($\lambda_{\text{ex}} = 381 \text{ nm}$, slits: ex = 5 nm, em = 3 nm).

Fig. 3. Emission spectra of **2** ($1 \times 10^{-5} \text{ mol/L}$) with different concentration of 2,4-dinitrophenylhydrazine added in CH_3CN at 25 °C. The concentrations of 2,4-dinitrophenylhydrazine for curves 1 to 21 were 0, 0.11, 0.33, 0.55, 0.80, 1.0, 1.25, 2.0, 2.7, 3.6, 6, 10, 12, 16, 20, 23, 27, 30, 36, 42, $45 \times 10^{-5} \text{ mol/L}$ (from top to bottom). ($\lambda_{\text{ex}} = 381 \text{ nm}$, slits: ex = 5 nm, em = 3 nm). Inset: the fluorescence of **2** as a function of C_{DNP}/C_2 at 439 nm.

3.4. Interactions of 2,4-dinitrophenylhydrazine (DNP) with **2**

In the forcpate structure of **2**, oxygen atom, hydrogen atom and nitrogen atom were possible binding sites for 2,4-dinitrophenylhydrazine (DNP). To understand the binding mode between **2** and DNP, ^1H NMR titration experiments were carried out

(Fig. 4). The proton signals on the benzene ring of 2,4-dinitrophenylhydrazine (DNP) in **2**·DNP underwent upfield shifting (*ca.* 0.02 ppm for H_{B1} , H_{B2} and H_{B3}) (Fig. 4(vi)), but the signals of protons of -NH-NH₂ on DNP didn't change, which indicated that -NO₂ of DNP participated in interactions between **2** and DNP, instead of -NH-NH₂. Meanwhile, the H_{A1} on NH beside anthracene ring of **2** was upfield shifted by 0.04 ppm (Fig. 4(vi)), which should be attributed to N-H···O interactions between DNP and NH of **2** (Scheme 2). H_{A7} and H_{A8} were upfield shifted 0.02 ppm. These shifts should be originated from the electron-donating effect of nitro group, in which amide was a strong electron-withdrawing group due to the high electronegativity of nitrogen atom and the influence of carbonyl. The proton signal of H_{A3} on the imidazole ring of **2** was downfield shifted by 0.05 ppm (Fig. 4(vi)), which should be originated from C-H···O interactions between DNP and imidazole rings of **2**. Also, the proton signals of H_{A2} , H_{A4} , H_{A5} and H_{A6} were downfield shifted by *ca.* 0.02 ppm. These shifts should be ascribed to the electron-withdrawing effect of nitro groups, in which the imidazolium ring is electron-donating unit because it contains one electron-rich π_{S} bond. Besides, no obvious change for other proton signals was observed, which showed that DNP was captured by C-H···O and N-H···O interactions. In addition, the proton signals of H_{A1} - H_{A8} had no notable change upon the addition of more DNP (Fig. 4(vii) and Fig. 4(viii)), and this indicated that **2** and DNP have a 1:1 complexation.

In Fig. S7, *m/z* (367.41) of **2**·DNP was observed, and it further proved the 1:1 complex between **2** and DNP. This result was consistent with the Job's plot experiment as shown in Fig. S5.

In the IR spectra of DNP, **2** and **2**·DNP, the bending vibration of $\nu(\text{C}=\text{N})$ moved from 1549 cm⁻¹ in free **2** to 1554 cm⁻¹ in **2**·DNP (Fig. S8), the $\nu(\text{N-H})$ absorption band moved from 740 cm⁻¹ in free **2** to 744 cm⁻¹ in **2**·DNP. The two absorption bands of nitro group moved from 1639 cm⁻¹ and 1321 cm⁻¹ in free 2,4-dinitrophenylhydrazine to 1647 cm⁻¹ and 1333 cm⁻¹ in **2**·DNP, respectively.

By analyzing the structure of **2**, ¹H NMR spectra, HRMS and IR spectra, the binding force between DNP and **2** turned out to be C-H···O and N-H···O interactions.

Because the imidazolium moieties are electron-rich groups and the amide groups are electron-withdrawing groups, the nitro groups have an electron-withdrawing effect on the imidazolium moieties and have an electron-donating effect on amide groups. When DNP was captured by **2**, the photoinduced electron transfer (PET) process from imidazolium moieties to anthracene ring was switch-on due to the influence of nitro groups [50]. As a result, fluorescence intensity of **2** decreased remarkably.

Scheme 2. The interactions of 2,4-dinitrophenylhydrazine (DNP) and **2**.

Fig. 4. The partial ^1H NMR spectra (DMSO- d_6 , 400 MHz) of DNP, **2** and **2**·DNP. (i) DNP only; (ii) **2** only; (iii) 0.25 equiv. of DNP and **2**; (iv) 0.5 equiv. of DNP and **2**; (v) 0.75 equiv. of DNP and **2**; (vi) 1 equiv. of DNP and **2**; (vii) 2 equiv. of DNP and **2**; (viii) 3 equiv. of DNP and **2**.

3.5. Recognition of 2,4-dinitrophenylhydrazine (DNP) using **3** as a host

The recognition of **3** for DNP was investigated with the analogous method to **2** (Fig. S9-Fig. S14). In ^1H NMR titration experiments of **3**, the proton signals of **3** and DNP were similar to the cases of **2** (Fig. S15), which indicated that DNP was also captured by **3** via C-H \cdots O and N-H \cdots O interactions (Scheme S1). The HRMS of **3**·DNP, and IR spectra of DNP, **3** and **3**·DNP were also measured. In the HRMS of **3**·DNP as displayed in Fig. S16, m/z (339.36) of **3**·DNP was observed, and this further proved a 1:1 complexation stoichiometry between **3** and DNP. IR spectra of **3**·DNP (Fig. S17) was similar to those of **2**·DNP (Fig. S8). The above experimental results indicated that **3** could also effectively discriminate DNP from other aromatic compounds through the method of fluorescence.

4. Conclusion

In summary, three bis-imidazolium salts **1-3** have been prepared and characterized. The structure of **1** was confirmed through X-ray analysis. The experimental results

showed that **2** (or **3**) had special selectivity for 2,4-dinitrophenylhydrazine (DNP), and they could effectively discriminate DNP from other aromatic compounds via the method of fluorescence. The K_{SV} value of $5.6 \times 10^4 \text{ M}^{-1}$ for **2**·DNP and $4.5 \times 10^4 \text{ M}^{-1}$ for **3**·DNP were obtained through a 1:1 association equation by using the method of fluorescence titration. The detection of **2** (or **3**) for DNP was of high sensitivity with the detection limits of $3.97 \times 10^{-10} \text{ mol/L}$ for **2** and $2.58 \times 10^{-10} \text{ mol/L}$ for **3**. By comparing, we found that the association constants and detection limits of **2** and **3** for DNP were similar, which displayed that the sizes of side chains (ⁿBu for **2** and Et for **3**) had no obvious effect on the recognition of the host toward DNP. The high sensitivity, selectivity and great affinity for DNP indicated that **2** (or **3**) could effectively discriminate DNP from other aromatic compounds. So, **2** (or **3**) might have potential application for distinguishing 2,4-dinitrophenylhydrazine from other aromatic compounds. The research of developing novel chemosensors for other nitro-aromatic compounds is underway.

Supporting Information

Tables, figures, fluorescence for **2**, **2**·DNP (or **3**, **3**·DNP) with this paper can be found in the online version.

ACKNOWLEDGMENTS

Financial supports for this work were by Tianjin Natural Science Foundation (No. 18JCZDJC99600), the National Natural Science Foundation of China (No. 21572159) and the Program for Innovative Research Team in University of Tianjin (TD13-5074).

References

- [1] J.S. Fan, Y.Z. Sun, X.Y. Li, C.L. Zhao, D.X. Tian, L.Y. Shao, J.X. Wang, Pollution of organic compounds and heavy metals in a coal gangue dump of the Gequan Coal Mine, China, *Chin. J. Geochem.* 2013;32:241-7.
- [2] L. Geng, G.B. Lv, C. Yong, H. Yin, D.Z. Dan, Determination of polycyclic aromatic hydrocarbons in sediment by high performance liquid chromatography

following vortex-assisted extraction combined with dispersive liquid-liquid microextraction, *Chinese J. Anal. Chem.* 2012;40:1752-7.

[3] Y.Z. Yang, N.M. Peleato, R.L. Legge, R.C. Andrews, Fluorescence excitation emission matrices for rapid detection of polycyclic aromatic hydrocarbons and pesticides in surface waters, *Environ. Sci.: Water Res. Technol.* 2019;5:315-24.

[4] Y.Q. Xie, B.N. Li, L.L. Liu, J. Ouyang, Y.W. Wu, Rapid screening of mineral oil aromatic hydrocarbons (MOAH) in grains by fluorescence spectroscopy, *Food Chem.* 2019;294:458-67.

[5] N. Howaniec, P. Kuna-Gwózdziwicz, A. Smolński, Assessment of emission of selected gaseous components from coal processing waste storage site, *Sustain.* 2018;10:744-51.

[6] F. Wei, X.Y. Cai, J.Q. Nie, F.Y. Wang, C.F. Lu, G.C. Yang, Z.X. Chen, C. Ma, Y.X. Zhang, A 1,2,3-triazolyl based conjugated microporous polymer for sensitive detection of p-nitroaniline and Au nanoparticles immobilization, *Polym. Chem.* 2018;9:3832-9.

[7] B.S. Kulkarni, V.N. Acharya, R.M. Khanna, S. Nath, R.P. Mankodi, P. Raghavan, Methemoglobinemia due to nitro-aniline intoxication. Review of the literature with a report of 9 cases, *J. Postgrad. Med.* 1969;15:192-200.

[8] M.T.D. Cronin, B.W. Gregory, T.W. Schultz, Quantitative structure-activity analyses of nitrobenzene toxicity to *tetrahymena pyriformis*, *Chem. Res. Toxicol.* 1998;11:902-8.

[9] Z. Li, M. Fang, M.K. Lagasse, J.R. Askim, K.S. Suslick, Colorimetric recognition of aldehydes and ketones, *Angew. Chem., Int. Ed.* 2017;56:9860-3.

[10] J.H. Wang, G.Y. Li, X.J. Liu, R. Feng, H.J. Zhang, S.Y. Zhang, Y.H. Zhang, A fluorescent anthracene-based metal-organic framework for highly selective detection of nitroanilines, *Inorganica Chimica Acta* 2018;473:70-4.

[11] A. Deshmukh, S. Bandyopadhyay, A. James, A. Patra, Trace level detection of nitroanilines using a solution processable fluorescent porous organic polymer, *J. Mater. Chem. C* 2016;4:4427-33.

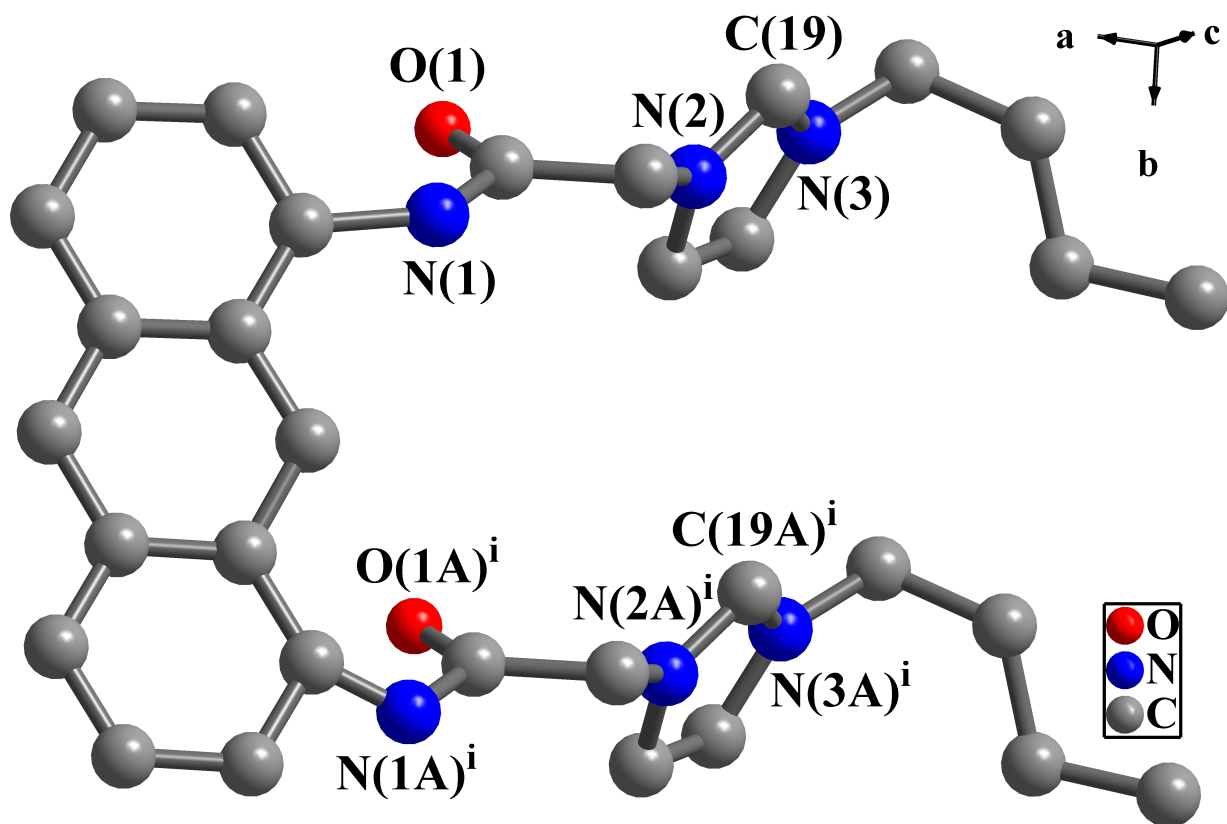
[12] A. Niazi, J. Ghasemi, A. Yazdanipour, Simultaneous spectrophotometric

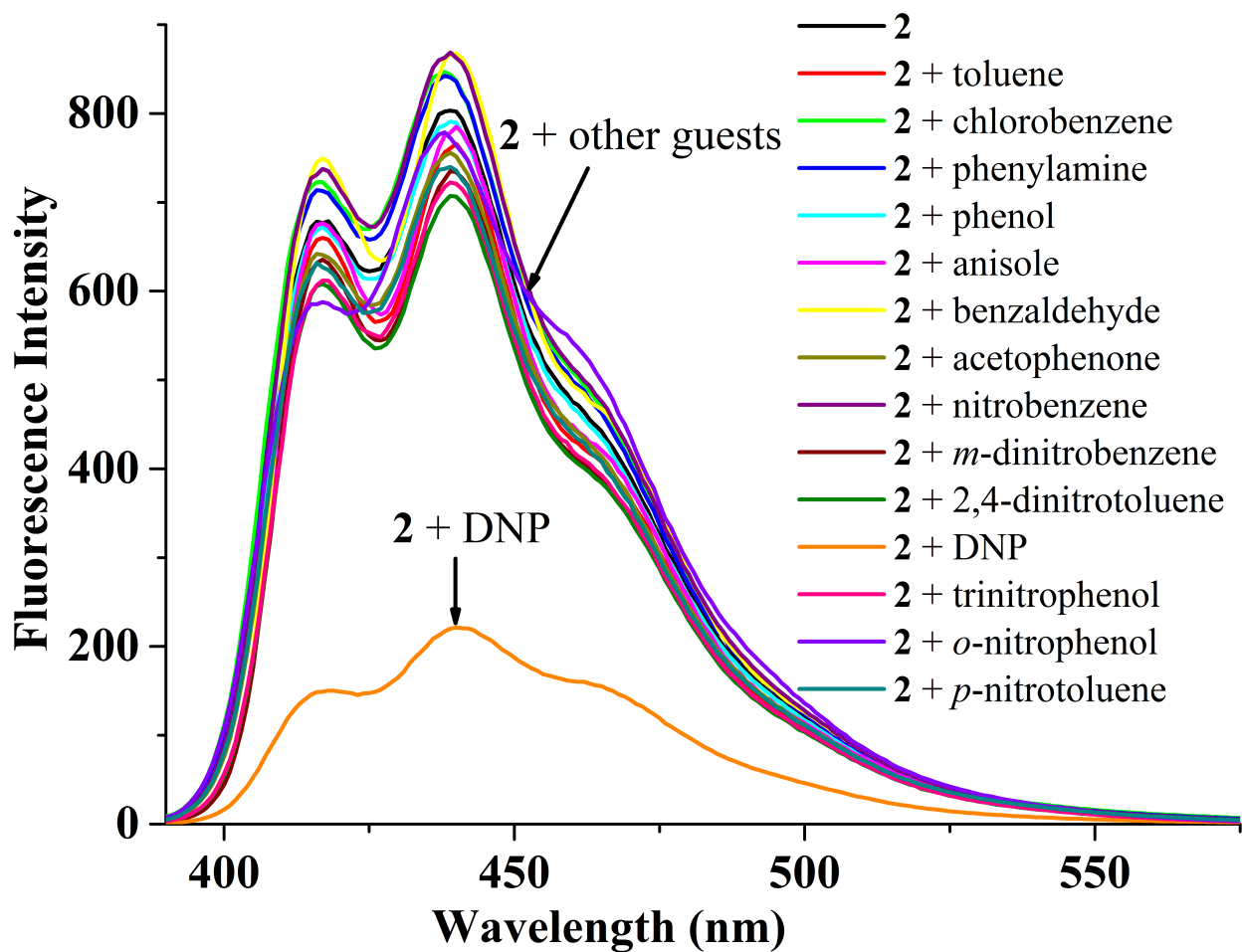
- determination of nitroaniline isomers after cloud point extraction by using least-squares support vector machines, *Spectrochim. Acta Part A* 2007;68:523-30.
- [13] R.P. Mu, H.L. Shi, Y. Yuan, A. Karnjanapiboonwong, J.G. Burken, Y.F. Ma, Fast separation and quantification method for nitroguanidine and 2,4-dinitroanisole by ultrafast liquid chromatography-tandem mass spectrometry, *Anal. Chem.* 2012;84:3427-32.
- [14] M. Berg, J. Bolotin, T.B. Hofstetter, Compound-specific nitrogen and carbon isotope analysis of nitroaromatic compounds in aqueous samples using solid-phase microextraction coupled to GC/IRMS, *Anal. Chem.* 2007;79:2386-93.
- [15] M. Najarro, M.E.D. Morris, M.E. Staymates, R. Fletcher, G. Gillen, Optimized thermal desorption for improved sensitivity in trace explosives detection by ion mobility spectrometry, *Analyst* 2012;137:2614-22.
- [16] P. Sulzer, F. Petersson, B. Agarwal, K.H. Becker, S. Jurschik, T.D. Mark, D. Perry, P. Watts, C.A. Mayhew, Proton transfer reaction mass spectrometry and the unambiguous real-time detection of 2,4,6-trinitrotoluene, *Anal. Chem.* 2012;84:4161-6.
- [17] S.J. Guo, D. Wen, Y.M. Zhai, S.J. Dong, E.K. Wang, Platinum nanoparticle ensemble-on-graphene hybrid nanosheet: one-pot, rapid synthesis, and used as new electrode material for electrochemical sensing, *ACS Nano* 2010;4:3959-68.
- [18] T.H. Kim, B.Y. Lee, J. Jaworski, K. Yokoyama, W.J. Chung, E. Wang, S. Hong, A. Majumdar, S.W. Lee, Selective and sensitive TNT sensors using biomimetic polydiacetylene-coated CNT-FETs, *ACS Nano* 2011;5:2824-30.
- [19] H. Ko, S. Chang, V.V. Tsukruk, Porous substrates for label-free molecular level detection of nonresonant organic molecules, *ACS Nano* 2009;3:181-8.
- [20] Y. Salinas, R. Martinez-Manez, M.D. Marcos, F. Sancenon, A.M. Costero, M. Parra, S. Gil, Optical chemosensors and reagents to detect explosives, *Chem. Soc. Rev.* 2012;41:1261-96.
- [21] S.S. Nagarkar, B. Joarder, A.K. Chaudhari, S. Mukherjee, S.K. Ghosh, Highly selective detection of nitro explosives by a luminescent metal-organic framework, *Angew. Chem., Int. Ed.* 2013;52:2881-5.

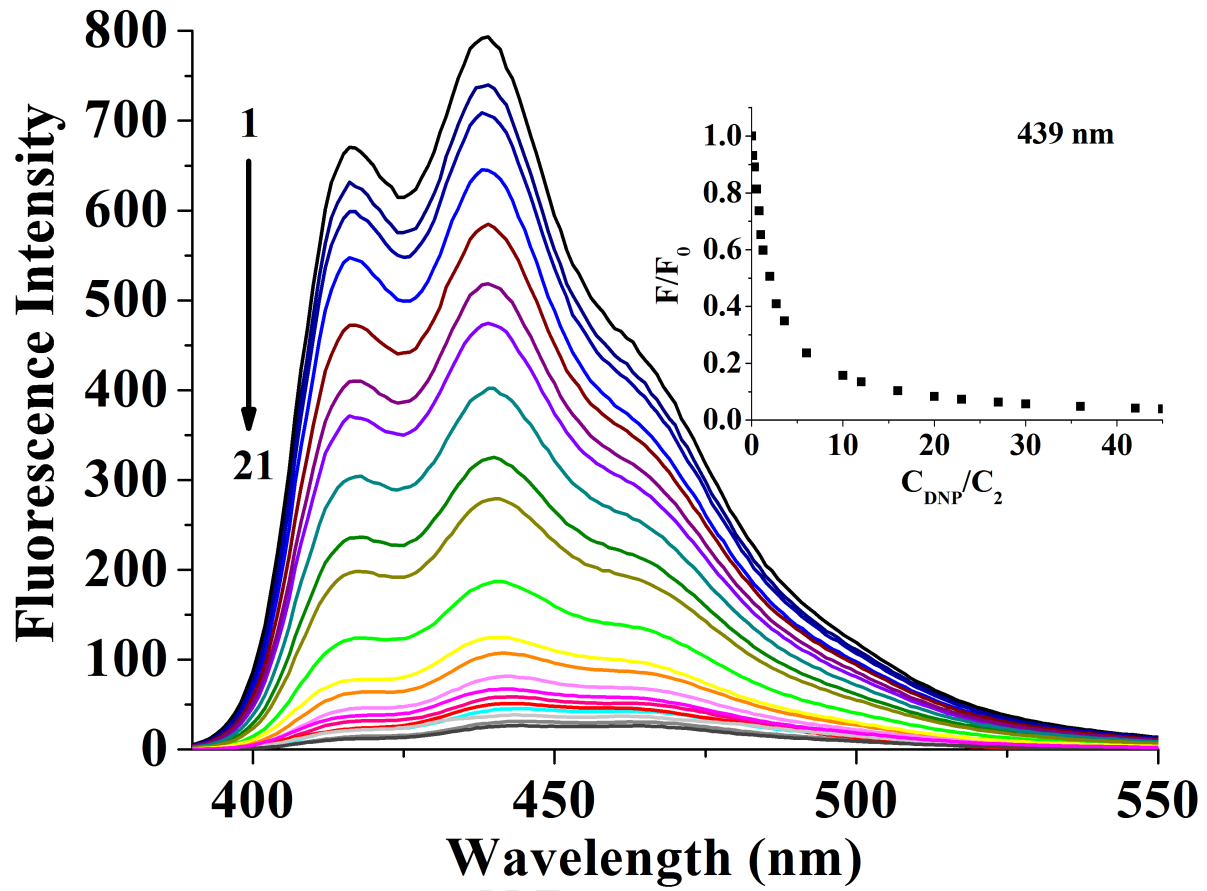
- [22] A.J. Lan, K.H. Li, H.H. Wu, D.H. Olson, T.J. Emge, W. Ki, M.C. Hong, J. Li, A luminescent microporous metal-organic framework for the fast and reversible detection of high explosives, *Angew. Chem., Int. Ed.* 2009;48:2334-8.
- [23] L.B. Sun, H.Z. Xing, J. Xu, Z.Q. Liang, J.H. Yu, R.R. Xu, A novel (3,3,6)-connected luminescent metal-organic framework for sensing of nitroaromatic explosives, *Dalton Trans.* 2013;42:5508-13.
- [24] M. Guo, Z.M. Sun, Solvents control over the degree of interpenetration in metal-organic frameworks and their high sensitivities for detecting nitrobenzene at ppm level, *J. Mater. Chem.* 2012;22:15939-46.
- [25] Z.J. Zhang, S.C. Xiang, X.T. Rao, Q. Zheng, F.R. Fronczek, G.D. Qian, B.L. Chen, A rod packing microporous metal-organic framework with open metal sites for selective guest sorption and sensing of nitrobenzene, *Chem. Commun.* 2010;46:7205-7.
- [26] R.B. Fu, S.M. Hu, X.T. Wu, Syntheses, crystal structures, thermal stabilities and luminescence of two metal phosphonates, *CrystEngComm* 2012;14:3478-83.
- [27] T.K. Kim, J.H. Lee, D. Moon, H.R. Moon, Luminescent Li-based metal-organic framework tailored for the selective detection of explosive nitroaromatic compounds: direct observation of interaction sites, *Inorg. Chem.* 2013;52:589-95.
- [28] X.H. Zhou, H.H. Li, H.P. Xiao, L. Li, Q. Zhao, T. Yang, J.L. Zuo, W. Hang, A microporous luminescent europium metal-organic framework for nitro explosive sensing, *Dalton Trans.* 2013;42:5718-23.
- [29] A. Laguerre, L. Stefan, M. Larrouy, D. Genest, J. Novotna, M. Pirrotta, D. Monchaud, A twice-assmart synthetic G-quartet: pyroTASQ is both a smart quadruplex ligand and a smart fluorescent probe, *J. Am. Chem. Soc.* 2014;136:12406-14.
- [30] Z.R. Dai, G.B. Ge, L. Feng, J. Ning, L.H. Hu, Q. Jin, D.D. Wang, X. Lv, T.Y. Dou, J.N. Cui, L. Yang, A highly selective ratiometric two-photon fluorescent probe for human cytochrome P450 1A, *J. Am. Chem. Soc.* 2015;137:14488-95.
- [31] B. Shi, Z.Y. Zhang, Q.Q. Jin, Z.Q. Wang, J. Tang, G. Xu, T. L. Zhu, X.Q. Gong, X.J. Tang, C.C. Zhao, Selective tracking of ovarian-cancer-specific

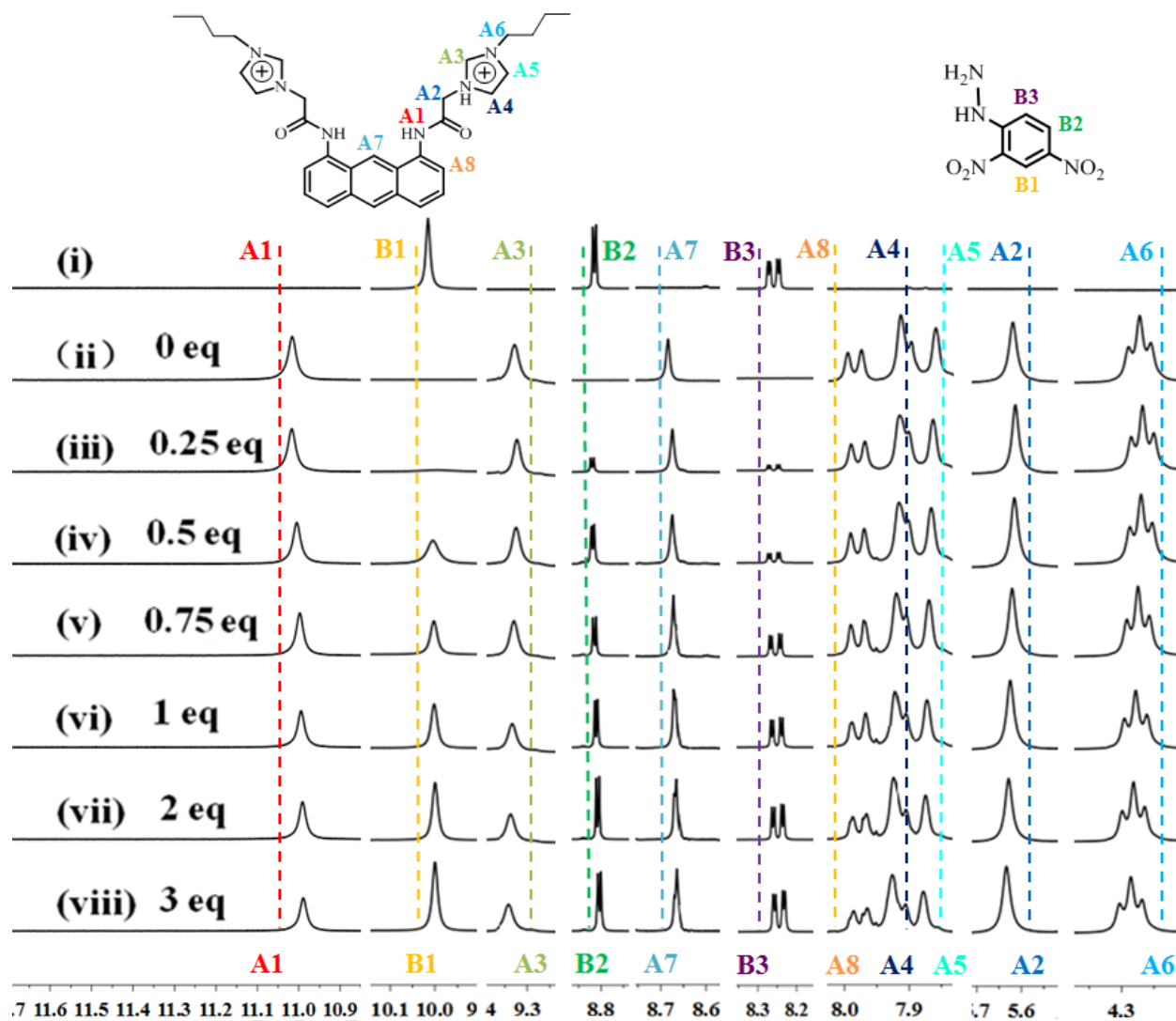
- γ -glutamyltranspeptidase using a ratiometric two-photon fluorescent probe, *J. Mater. Chem. B* 2018;6:7439-43.
- [32] A.X.S. Bruker, SAINT Software Reference Manual, Madison, WI. 1998.
- [33] G.M. Sheldrick, SHELXTL NT (Version 5.1), Program for Solution and Refinement of Crystal Structures, University of Göttingen, Göttingen (Germany). 1997.
- [34] D.C. Palmer, Crystal Maker 7.1.5, CrystalMaker Software, Yarnton, UK. 2006.
- [35] Z. Lu, S.A. Cramer, D.M. Jenkins, Exploiting a dimeric silver transmetallating reagent to synthesize macrocyclic tetracarbene complexes, *Chem. Sci.* 2012;3:3081-7.
- [36] D.T. Weiss, S. Haslinger, C. Jandl, A. Pothig, M. Cokoja, F.E. Kühn, Application of open chain tetraimidazolium salts as precursors for the synthesis of silver tetra (NHC) complexes, *Inorg. Chem.* 2015;54:415-7.
- [37] B. Liu, X.J. Ma, F.F. Wu, W.Z. Chen, Simple synthesis of neutral and cationic Cu-NHC complexes, *Dalton Trans.* 2015;44:1836-44.
- [38] B. Liu, S.F. Pan, B. Liu, W.Z. Chen, Di-, tri-, and tetranuclear copper (I) complexes of phenanthroline-linked dicarbene ligands, *Inorg. Chem.* 2014;53:10485-97.
- [39] Q.X. Liu, Q. Wei, R. Liu, X.J. Zhao, Z.X. Zhao, NHC macrometalloacycles of mercury(II) and silver(I): synthesis, structural studies and recognition of Hg(II) complex 4 for silver ion. *RSC. Adv.* 2015;5:28435-47.
- [40] Q.X. Liu, A.H. Chen, X.J. Zhao, Y. Zang, X.M. Wu, X.G. Wang, J.H. Guo, N-Heterocyclic carbene copper(I), mercury(II) and silver(I) complexes containing durene linker: synthesis and structural studies. *CrystEngComm* 2011;13:293-305.
- [41] M.L. Cole, P.C. Junk, Facile purification of the N-heterocyclic carbene precursor [IMesH][Cl] and chloride binding in the solvates [IMesH][Cl]·acetone and [IMesH][Cl]·H₂O (IMes = 1,3-bis(2,4,6-trimethylphenyl)imidazol-2-ylidene), *CrystEngComm* 2004;6:173-6.
- [42] F. Zhang, L. Luo, Y. Sun, F.J. Miao, J.H. Bi, S.L. Tan, D.M. Tian, H.B. Li, Synthesis of a novel fluorescent anthryl calix [4] arene as picric acid sensor, *Tetrahedron* 2013;69:9886-9.

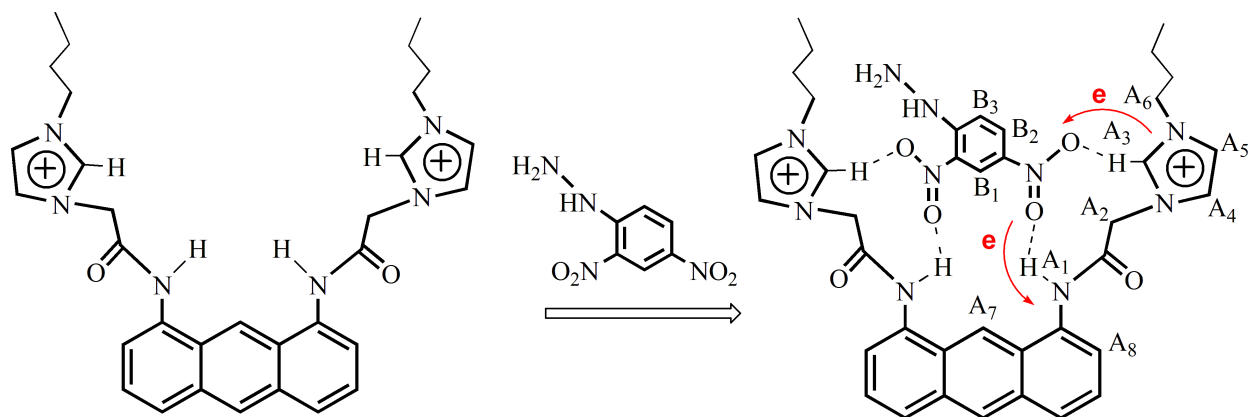
- [43] C. Chang, F. Wang, J. Qiang, Z. Zhang, Y. Chen, W. Zhang, Y. Wang, X. Chen, Benzothiazole-based fluorescent sensor for hypochlorite detection and its application for biological imaging, *Sens. Actuators B* 2017;243:22-8.
- [44] Y.J. Gong, X.B. Zhang, C.C. Zhang, A.L. Luo, T. Fu, W. Tan, G.L. Shen, R.Q. Yu, Through bond energy transfer: A convenient and universal strategy toward efficient ratiometric fluorescent probe for bioimaging applications, *Anal. Chem.* 2012;84:10777-84.
- [45] E.S. Zhang, P. Ju, Z. Zhang, H. Yang, L. Tang, X.Y. Hou, J.M. You, J.J. Wang, A novel multi-purpose Zn-MOF fluorescent sensor for 2,4-dinitrophenylhydrazine, picric acid, La^{3+} and Ca^{2+} : Synthesis, structure, selectivity, sensitivity and recyclability, *Spectrochim. Acta Part A* 2019;222:117207.
- [46] Q.Y. Wang, X.H. Wang, Y.W. Wu, Highly sensitive and selective fluorescence probe for 2,4-dinitrophenylhydrazine detection in wastewater using water-soluble CdTe QDs, *Photochem. Photobiol.* 2019;95:895-900.
- [47] A. Caballero, R. Martinez, V. Lloveras, I. Ratera, J. Vidal-Gancedo, K. Wurst, A. Tarraga, P. Molina, J.J. Veciana, Highly selective chromogenic and redox or fluorescent sensors of Hg^{2+} in aqueous environment based on 1,4-disubstituted azines, *J. Am. Chem. Soc.* 2005;127:15666-7.
- [48] S. Li, D. Zhang, X.Y. Xie, S.G. Ma, Y. Liu, Z.H. Xu, Y.F. Gao, Y. Ye, A novel solvent-dependently bifunctional NIR absorptive and fluorescent ratiometric probe for detecting $\text{Fe}^{3+}/\text{Cu}^{2+}$ and its application in bioimaging, *Sens. Actuators B*, 2016;224:661-7.
- [49] J.Y. Cheng, E.B. Yang, P.G. Ding, J. Tang, D. Zhang, Y.F. Zhao, Y. Ye, Two rhodamine based chemosensors for Sn^{4+} and the application in living cells, *Sens. Actuators B*, 2015;221:688-93.
- [50] D. Escudero, Revising intramolecular photoinduced electron transfer (PET) from first-principles, *Acc. Chem. Res.* 2016;49:1816-24.











Journal Pre-proof

- Three bis-imidazolium salts **1-3** have been prepared and characterized.
- The structure of **1** was confirmed through X-ray analysis.
- **2** (or **3**) had high sensitivity and selectivity, and great affinity for 2,4-dinitrophenylhydrazine (DNP), and can effectively discriminate from DNP and other aromatic compounds via the method of fluorescence.
- The K_{SV} value of $5.6 \times 10^4 \text{ M}^{-1}$ for **2**·DNP and $4.5 \times 10^4 \text{ M}^{-1}$ for **3**·DNP
- The detection limits are $3.97 \times 10^{-10} \text{ mol/L}$ for **2** and $2.58 \times 10^{-10} \text{ mol/L}$ for **3**.

Conflicts of interest

There are no conflicts to declare.

Journal Pre-proof